

## PATHWAYS FOR RETINAL DEPROTONATION IN BACTERIORHODOPSIN

ANA-NICOLETA BONDAR

*Computational Molecular Biophysics, IWR, University of Heidelberg,  
Im Neuenheimer Feld 368, D-69120 Heidelberg, Germany  
E-mail: nicoleta.bondar@iwr.uni-heidelberg.de*

(Received August 16, 2005)

*Abstract.* The transfer of the retinal Schiff base proton to Asp85 is an essential step in the bacteriorhodopsin photocycle. Here, we review recent Quantum Mechanical/Molecular Mechanical reaction pathway calculations on the mechanism of retinal deprotonation, discussing the compatibility of various retinal configurations with a proton-pumping photocycle. The role of specific protein groups for the stability of the ion-pair state (*i.e.*, the state with protonated Schiff base and negatively charged Asp85) is also considered.

*Key words:* bacteriorhodopsin, proton transfer, QM/MM, reaction pathways.

### 1. INTRODUCTION

The active transport of protons across biological membranes is essential for many cellular processes. Bacteriorhodopsin, a light-driven proton pump found in the plasma membrane of *Halobacterium Salinarium* [1], is perhaps the best studied cellular ionic pump. Bacteriorhodopsin consists of seven transmembrane helices labeled A-G. The retinal chromophore is covalently attached to Lys216 on helix G via a protonated Schiff base. In the initial, ground state bR retinal has an all-*trans* configuration. Upon absorption of light retinal isomerizes to 13-*cis* and the K intermediate forms on the picosecond timescale. Following the decay of K into L in  $\sim 1 \mu\text{s}$ , a first proton transfer step occurs between the L and M intermediates on the  $\sim 10 \mu\text{s}$  timescale. During this primary transfer step, the retinal Schiff base proton is transferred to the nearby Asp85 amino-acid residue. Four additional proton-transfer steps occur, resulting in the net transfer of one proton from the cytoplasmic to the extracellular side of the membrane. Thus, bacteriorhodopsin converts the energy of the absorbed light into an electrochemical gradient that is used by the cell to synthesise ATP (for recent reviews see [2–4]).

Several scenarios have been proposed to explain how retinal deprotonation takes place [see, *e.g.*, 2, 3, 5, 6]. Depending on the geometry of the retinal and the

protein groups in its immediate vicinity, the proton may be transferred directly to Asp85 or *via* an intermediate carrier mechanism involving specific water molecules and/or protein groups. The debate over the mechanism of the first proton transfer step is due to controversies regarding the structural details of the L intermediate, *i.e.*, the intermediate that is ready for the first proton transfer step. Although the global protein structures are similar, the retinal configurations indicated in three L-state crystal structures are very different [7–9]. In two of these crystal structures [7, 9] the Schiff base of the 13-*cis*, 15-*anti* retinal points towards the cytoplasmic side, whereas in the third one [8] the Schiff base of the twisted 13-*cis*, 15-*syn* retinal points in the opposite direction, towards the extracellular side of the membrane. These different orientations of the retinal Schiff base (the proton donor group) relative to Asp85 (the proton acceptor group), may lead to different proton transfer pathways. Due to the difficulties in experimentally characterizing the transition states associated with the proton transfer reaction, the atomic details of the mechanism by which the first proton transfer step occurs are not completely understood.

## 2. COMPUTER SIMULATIONS ON THE RETINAL DEPROTONATION STEP

The theoretical investigation of proton transfer pathways in a complex biochemical system such as bacteriorhodopsin is computationally demanding. The reacting partners (*i.e.*, the proton donor and acceptor groups) must be treated with quantum mechanical methods that can accurately describe the breaking and forming of chemical bonds. Due to the computational costs, one cannot treat the entire protein using quantum mechanical methods. As a solution one can use the combined Quantum Mechanical/Molecular Mechanical (QM/MM) approach, where only the active site is treated with quantum mechanical methods and the remaining part of the protein is treated with classical mechanics [10–12]. In our QM/MM investigations of bacteriorhodopsin proton transfer [13–17] we employed the approximate self-consistent-charge density functional tight-binding (SCC-DFTB) method [18] for all path optimizations. The optimized low-energy reaction pathways were further refined by performing energy calls using the B3LYP functional [19–20] with the 6-31G\*\* basis set. The interactions between the classical atoms were computed using the CHARMM force field [21]. The QM:MM interactions were computed as described previously [12, 22]. The quantum mechanical region consisted of retinal, the side-chain of Lys216, Asp85 and Asp212, as well as water molecule w402 that is located between Asp85 and Asp212. Hydrogen link atoms [12] were attached to the C<sub>γ</sub> atom of Lys216 and to the C<sub>β</sub> atoms of Thr89, Asp85, and Asp212.

Since experiments indicate that the retinal deprotonation step is dominated by enthalpy [23] and no significant protein conformational changes occur in the first half of the photocycle [24], as a first approximation we computed potential energy

barriers. The minimum energy pathways connecting the reactant (protonated Schiff base and negatively charged Asp85) to the product state (neutral Schiff base and Asp85) structures were computed using the conjugate peak refinement algorithm (CPR, [25]) as implemented in the TRAVEL module of CHARMM [21]. Starting from energy-optimized reactant and product state structures, and without the *a priori* definition of a reaction coordinate, CPR finds a minimum-energy pathway along which the energy maxima are first-order saddle points that give the transition states of the reaction.

### 3. MECHANISM OF RETINAL DEPROTONATION

Knowledge of the retinal configuration in the L intermediate is essential for understanding the pathway followed by the Schiff base proton. An exhaustive computation of the pathways for transitions between various retinal states [13, 14, 26] led to the unexpected conclusion that prior to deprotonation the retinal Schiff base points to the cytoplasmic side of the membrane, *i.e.*, in the direction opposite to the net proton transfer. Starting from this initial state and within the error associated with our calculations three proton transfer routes were found that are almost isoenergetic and have barriers consistent with the experimental enthalpy of activation [23]. One of these is a direct proton transfer from the retinal Schiff base to Asp85, with a 12.4 kcal/mol rate-limiting barrier. This transfer path requires significant twisting in the retinal chain and flexibility in helix C containing Asp85, as suggested previously [6]. The second pathway, which has been suggested previously [5, 6] involves the concerted transfer of the Schiff base proton to Thr89 and of the Thr89 hydroxyl proton to Asp85. The Thr89 pathway, with a 13.6 kcal/mol associated rate-limiting barrier, does not require any significant structural rearrangements. In the third pathway, following the reorientation of the retinal Schiff base towards Asp212 the proton is first transferred to Asp212 (Fig. 1C) and then to Asp85 through a proton wire that is formed with the help of water w402 (Fig. 1D). The transfer of the Schiff base proton to Asp212 gives the rate-limiting barrier, which is 11.5 kcal/mol above the cytoplasmic-oriented initial state.

The existence of a 13,14-*dicis* retinal configuration prior to the first proton transfer step has been the subject of debate [27–29]. Starting from the QM/MM-optimized 13,14-*dicis* retinal model we computed the pathway for proton transfer *via* water w402 [13]. The rate-limiting step of the reaction is given by the rearrangement of water w402 such that it can receive the Schiff base proton (Fig. 1E). Further rearrangement of water w402 leads to a configuration from which the Schiff base proton is transferred to water w402, followed by the transfer of one proton from w402 to Asp85.

Relative to the low-energy, cytoplasmic-oriented initial state, there is a 14.1 kcal/mol rate-limiting barrier associated with the deprotonation of the 13,14-*dicis*

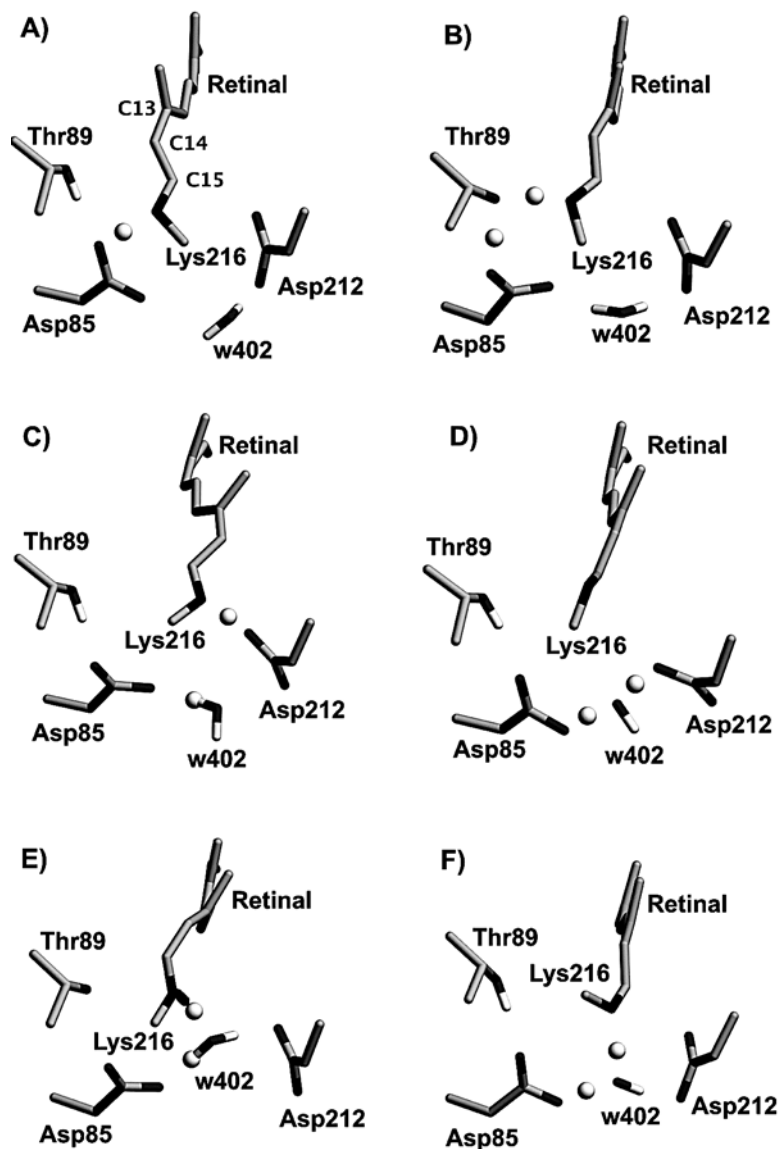


Fig. 1 – Pathways for retinal deprotonation in bacteriorhodopsin. The saddle-point configuration of the retinal and protein groups in the close vicinity is shown for (A) the direct proton transfer; (B) proton transfer *via* Thr89; (C-D) proton transfer *via* Asp212 and water w402; proton transfer *via* w402 starting from the 13,14-*dicis* retinal (E) and the 13-*cis*, 15-*syn* retinal (F). Only retinal and protein groups treated with QM are depicted. The transferred protons are shown as small spheres.

retinal. This energy barrier is significantly higher than the  $< 3$  kcal/mol required for the 13,14-*dicis* retinal to relax to 13-*cis*, 14-*trans* with the Schiff base NH bond

pointing towards the cytoplasmic side [13]. This indicates that the 13,14-*dicis* retinal is more likely to proceed with rapid relaxation to 13-*cis*, 14-*anti* than with proton transfer [13].

A recent crystallographic analysis of the L intermediate indicated a twisted 13-*cis*, 15-*syn* retinal configuration and a geometry of the retinal binding site that would suggest proton transfer *via* water w402 [8]. The proton-transfer pathway computed from the QM/MM-optimized 13-*cis*, 15-*syn* model occurs without any significant structural rearrangements. Although the 7.3 kcal/mol rate-limiting barrier associated with this proton-transfer scenario is smaller than for the three low-energy paths discussed above, the following considerations make the 13-*cis*, 15-*syn* pathway less likely to be followed. The deprotonated 13-*cis*, 15-*syn* retinal remains with the Schiff base pointing towards the extracellular side of the membrane, whereas a proton-pumping photocycle requires that following deprotonation the retinal Schiff base points towards the cytoplasmic side of the membrane, such that it can be reprotonated from Asp96. The transition of the deprotonated retinal from 13-*cis*, 15-*syn*, extracellular-oriented, to 13-*cis*, 15-*anti*, cytoplasmic oriented is energetically unfavourable [13, 26], such that if the first proton transfer step would occur from 13-*cis*, 15-*syn*, the photocycle could not proceed with pumping. This unproductive pathway is avoided due to the high-energy barrier associated with the formation of 13-*cis*, 15-*syn* [13].

#### 4. UNDERSTANDING THE PROTON-TRANSFER ENERGY PROFILE

The intrinsic proton affinities of the proton donor and acceptor groups would make the ion-pair state extremely unfavorable [13, 26]. Indeed, in the case of the system composed only of the retinal and Asp85 with their coordinates selected from the QM/MM-optimized pathway, the energy profile (computed without energy optimization) indicates a 17.4 kcal/mol energy decrease upon proton transfer. In order to understand how the energy profile of the direct proton-transfer path is influenced by the interaction between the reacting pair and specific protein groups, we computed the energy profile by adding the following groups to the minimal system formed by the retinal and Asp85: *i*) Thr89, *ii*) Thr89 and Asp212, and *iii*) Thr89, Asp212 and water w402. Including Thr89 or Thr89 and Asp212 did not lead to a proton-transfer barrier, however the ion-pair state was stabilized by ~ 4 and respectively ~ 11 kcal/mol. When water w402 was added a ~ 5 kcal/mol energy barrier was obtained that is due to the breaking of the Asp85:w402 hydrogen bond during proton transfer. A detailed decomposition of QM/MM-optimized energy profile of the direct proton transfer pathway revealed the essential role of the QM:MM non-bonded interactions in determining the rate-limiting energy barrier [13].

## 5. CONCLUSION

In this review we discussed several aspects of the first proton transfer step in bacteriorhodopsin. The 13-*cis*, 15-*anti* retinal is compatible with an active photocycle regardless of the configuration about the C<sub>14</sub>-C<sub>15</sub> retinal bond. Three different pathways computed from the 13-*cis*, 14-*trans*, cytoplasmic-oriented retinal state have barriers consistent with the experimental enthalpy of activation [23]. Significant flexibility in the retinal chain and the protein environment may assist retinal deprotonation. The non-bonded interactions between the protein environment and the reacting partners have an essential role in determining the proton transfer energetics.

## REFERENCES

1. D. Oesterhelt and W. Stoerkenius, Functions of a new photoreceptor membrane, *Proc. Natl. Acad. Sci. USA*, 70, 2853–2854 (1973).
2. R. Neutze, E. Pebay-Peyroula, K. Edman, A. Royant, J. Navarro, and E. M. Landau, Bacteriorhodopsin: a high-resolution structural view of vectorial proton transport, *Biochim. Biophys. Acta*, 1565, 144–167 (2002).
3. J. K. Lanyi, Bacteriorhodopsin, *Annu. Rev. Physiol.*, 66, 665–688 (2004).
4. T. Hirai and S. Subramaniam, Structural insights into the mechanism of proton pumping by bacteriorhodopsin, *FEBS Letters*, 545, 2–8 (2003).
5. S. Subramaniam and R. Henderson, Molecular mechanism of vectorial proton translocation by bacteriorhodopsin, *Nature*, 406, 653–657 (2000).
6. K. Edman, A. Royant, G. Larsson, F. Jacobson, T. Taylor, D. van der Spoel, E. M. Landau, E. Pebay-Peyroula, and R. Neutze, Deformation of helix C in the low-temperature L-intermediate of bacteriorhodopsin, *J. Biol. Chem.*, 279, 2147–2158 (2004).
7. A. Royant, K. Edman, T. Ursby, E. Pebay-Peyroula, E.M. Landau, and R. Neutze, Helix deformation is coupled to vectorial proton transport in the photocycle of bacteriorhodopsin, *Nature*, 406, 645– (2000).
8. J. K. Lanyi and B. Schobert, Mechanism of the proton transport in bacteriorhodopsin from crystallographic structures of the K, L, M<sub>1</sub>, M<sub>2</sub>, and M<sub>2</sub>' intermediates of the photocycle, *J. Mol. Biol.*, 328, 439–450 (2003).
9. T. Kouyama, T. Nishikawa, T. Tokunisha, and H. Okumura, Crystal structure of the L intermediate of bacteriorhodopsin: evidence for vertical translocation of a water molecule during the proton pumping cycle, *J. Mol. Biol.*, 335, 531–546 (2004).
10. A. Warshel, Computer modeling of chemical reactions in enzymes and solutions. John Wiley and Sons, New York (1991).
11. U. C. Singh and P. Kollman, A combined ab initio quantum mechanical and molecular mechanical method for carrying out simulations on complex molecular systems: Applications to the CH<sub>3</sub>Cl+Cl<sup>-</sup> exchange reaction and gas phase protonation of polyethers, *J. Comput. Chem.*, 7, 718–730 (1986).
12. M. J. Field, P. A. Bash, and M. Karplus, A combined quantum mechanical and molecular mechanical potential for molecular dynamics simulations, *J. Comput. Chem.*, 11, 700–733 (1990).
13. A.-N. Bondar, S. Fischer, J. C. Smith, M. Elstner, and S. Suhai, Key role of electrostatic interactions in bacteriorhodopsin proton transfer, *J. Am. Chem. Soc.*, 126, 14668–14677 (2004).

14. A.-N. Bondar, M. Elstner, S. Suhai, J. C. Smith, and S. Fischer, Mechanism of bacteriorhodopsin proton transfer, *Structure* 12, 1281–1288 (2004).
15. N. Bondar, M. Elstner, S. Fischer, J. C. Smith, and S. Suhai, Can coordinate driving describe proton transfer coupled to complex protein motions? *Phase Transitions*, 77, 47–52 (2004).
16. A.-N. Bondar, M. Elstner, S. Suhai, S. Fischer, and J. C. Smith, Direct proton transfer in a putative L-state intermediate of the bacteriorhodopsin photocycle, *Phase Transitions*, 78, 5–9 (2005).
17. A.-N. Bondar, S. Fischer, S. Sihai, and J. C. Smith, Tuning of retinal twisting in bacteriorhodopsin controls the directionality of the early photocycle steps, *J. Phys. Chem. B.*, 2005, In Press.
18. M. Elstner, D. Porezaf, G. Jungnickel, J. Elner, M. Haugk, T. Frauenheim, S. Suhai, and G. Seifert, Self-consistent-charge density-functional tight-binding method for simulations of complex materials properties, *Phys. Rev. B*, 58, 7260–7268 (1998).
19. A. D. Becke, Density-functional exchange-energy approximation with correct asymptotic behaviour, *Phys. Rev. A*, 38, 3098–3100 (1988).
20. C. Lee, W. Yang, and R. G. Parr, Development of the Colle-Salvetti correlation-energy formula into a functional of the electron density, *Phys. Rev. B*, 37, 785–789.
21. B. R. Brooks, R. E. Bruccoleri, B. D. Olafson, D. J. States, S. Swaminathan, and M. Karplus, CHARMM: a program for macromolecular energy minimization and dynamics calculations, *J. Comput. Chem.*, 4, 187 (1983).
22. Q. Cui, M. Elstner, E. Kaxiras, T. Frauenheim, and M. Karplus, A QM/MM implementation of the Self-Consistent Charge Density Functional Tight Binding (SCC-DFTB) method, *J. Phys. Chem. B*, 105 569 (2001).
23. K. Ludman, C. Gergely, G. and Váró, Kinetic and thermodynamic study of the bacteriorhodopsin photocycle over a wide pH range, *Biophys. J.*, 75, 3110–3119 (1998).
24. S. Subramaniam, M. Lindahl, P. Bullough, A. R. Faruki, J. Tittor, D. Oesterhelt, L. Brown, J. K. Lanyi, and R. Henderson, Protein conformational changes in the bacteriorhodopsin photocycle, *J. Mol. Biol.*, 287, 145–161 (1999).
25. S. Fischer and M. Karplus, Conjugate Peak Refinement: an algorithm for finding reaction paths and accurate transition states in systems with many degrees of freedom, *Chem. Phys. Lett.*, 194, 252–261 (1992).
26. A. N. Bondar, Active ion transfer across cellular membranes: The mechanism of the bacteriorhodopsin proton pump, Dissertation, University of Heidelberg, 2004.
27. K. Schulten and P. Tavan, A mechanism for the light-driven proton pump of *Halobacterium Salinarium*, *Nature*, 272, 85–86 (1978).
28. K. Gerwert and F. Siebert, Evidence for light-induced 13-*cis*, 14-*s-cis* isomerization in bacteriorhodopsin obtained by FTIR difference spectroscopy using isotopically labeled retinals, *The EMBO J.* 5, 805–811 (1986).
29. S. P. A. Fodor, W. T. Pollard, R. Gebhard, E. M. van der Berg, J. Lugtenburg, and R. A. Mathies, Bacteriorhodopsin's L<sub>550</sub> intermediate contains a C14-C15 *s-trans*-retinal chromophore, *Proc. Natl. Acad. Sci. USA*, 85, 2156–2160 (1988).